Estimation of the Atrial Activity from Electrograms: A Beamforming Perspective

Tijs Moree[1], Mathijs S van Schie[2], Natasja MS de Groot[1,2], Richard C Hendriks[1]

[1] Delft University of Technology, Delft, the Netherlands
[2] Erasmus Medical Center, Rotterdam, the Netherlands

Abstract

Inspection of local atrial activity using atrial electrograms (EGMs) is important to determine the arrhythmogenic substrate underlying arrhythmias such as atrial fibrillation (AF). During AF, the atrial activity (AA) is often distorted by ventricular activity (VA). An effective means to remove this VA is to use a bipolar electrode configuration. However, this configuration distorts the AA as well.

In this paper, AA estimation is formulated as a beamforming problem, common in the field of array signal processing. We propose two different beamformers for AA estimation. Simulations are done with synthetically generated EGMs containing VA and various degrees of AF. Compared to the standard bipolar configuration, both the proposed estimators lead to significantly less distortion on the atrial component and a better removal of the ventricular component for scenarios with a relatively low degree of AF. The current signal model is, however, less suitable for scenarios with a higher degree of AF.

1. Introduction

Atrial fibrillation (AF) is the most common heart rhythm disorder. It increases the risk of heart failures and strokes and affects about 1–2% of the population [1]. The exact underlying mechanism of this disorder is still unknown. To gain knowledge on its origin, the heart muscle activity can be measured during open heart surgery using multiple electrodes, forming an atrial electrogram (EGM) [2].

These EGMs mostly consist of local atrial activity (AA), but they will be distorted with far-field ventricular activity (VA) as well. During sinus rhythm (SR) this generally is not a problem, because the AA and VA are temporally separated. However, during AF the AA and VA might overlap, resulting in EGMs that are harder to interpret. Bipolar electrode (BE) configurations, see e.g., [3], are often used to overcome this issue. However, this configuration results in direction dependent distortions on the AA as well.

The BE is also known as a differential beamformer from the field of array processing, see e.g., [4]. Although the BE only uses two electrodes, it is expected that using more than two electrodes and using more complex beamformer weights might lead to better results regarding the preservation of the AA and cancellation of the VA.

To get more insight on the possibilities of estimating the atrial component from EGMs, we make in this paper use of concepts from the field of array processing. We will formulate AA estimation as a beamforming problem and derive several beamformers for estimating the AA, based on various signal model assumptions. The bipolar electrode configuration follows as a special case.

2. Signal model and problem formulation

Let $X_m[t]$ denote an EGM measured at electrode $m \in \{1, ..., M\}$ and at time t, which is assumed to consist of three additive stochastic processes, that is,

$$X_m[t] = S_{a,m}[t] + S_{v,m}[t] + N_m[t], \quad (1)$$

where $S_{a,m}[t]$ and $S_{v,m}[t]$ are the processes of the atrial and the ventricular signal components respectively. Further, $N_m[t]$ is the noise process, which models the sensor self-noise and is considered to be a zero-mean white process with power spectral density (PSD) σ_n^2. The three processes are assumed to be mutually independent.

Furthermore, it is assumed that the stochastic atrial and ventricular components as observed at any electrode m can be modeled as $S_{a,m}[t] = (S_a * a_m)[t]$ and $S_{v,m}[t] = (S_v * v_m)[t]$ with $*$ being the temporal convolution. Here $S_a[t]$ and $S_v[t]$ are the atrial and ventricular sources and $a_m[t]$ and $v_m[t]$ are the impulse responses that model how the stereotypical sources $S_a[t]$ and $S_v[t]$ propagate from their (virtual) source locations to electrode m.

Notice that this thus implies that we assume that every electrode m observes the same atrial and ventricular sources $S_a[t]$ and $S_v[t]$, up to an electrode dependent convolution with the spatial impulse responses $a_m[t]$ and $v_m[t]$, respectively. Altogether, a realization of $X_m[t]$ is then given by

$$x_m[t] = (s_{a,t} * a_m)[t] + (s_{v,t} * v_m)[t] + n_m[t]. \quad (2)$$

We denote stochastic processes with uppercase symbols and their realizations with the corresponding lowercase symbols. Further, matrices and vectors are boldfaced.

When transforming Eq. (2) to the Fourier domain per time frame k and using a stacked vector notation across all M electrodes, we get,

$$\mathbf{x}(k, f) = s_a(k, f)\mathbf{a}(k, f) + s_v(k, f)\mathbf{v}(k, f) + \mathbf{n}(k, f), \quad (3)$$

with k and f the time frame and frequency band index, respectively, and where $\mathbf{x} \in \mathbb{C}^M$. As all processing will be done per k and f, we will from now on neglect the indices k and f for notational convenience. The symbols s_a and s_v denote the Fourier transforms of the atrial and ventricular sources, $\mathbf{a}$ and $\mathbf{v}$ denote the Fourier transforms of the aforementioned atrial and ventricular impulse responses, called the atrial and ventricular transfer functions, ATF and VTF respectively, and $\mathbf{n}$ denotes the vector containing the remaining noise.

The goal is to estimate the atrial component $\mathbf{s}_a = s_a\mathbf{a}$. We do this by first estimating the ATF $\mathbf{a}$ and then deriving a beamformer $\mathbf{w}$ such that $\hat{s}_a = \mathbf{w}^H\mathbf{x}$ with $(\cdot)^H$ being the Hermitian operator. Using $\mathbf{W} = \mathbf{wa}^H$, we obtain an estimate for all electrodes, that is,

$$\hat{\mathbf{s}}_a = \mathbf{W}^H\mathbf{x}. \quad (4)$$

3. Transfer function estimation

Estimating the ATF and VTF requires some more insight into the signal model. Similar to Eq. (3), the random processes in the Fourier domain are given by

$$\mathbf{X} = \mathbf{S}_a + \mathbf{S}_v + \mathbf{N}. \quad (5)$$

The spatial cross-correlation matrix is defined as $\mathbf{R_X} = \mathrm{E}\left[\mathbf{XX}^H\right]$, which simplifies due to the assumed mutually independence of the AA, the VA and the noise, into

$$\mathbf{R_X} = \mathbf{R_A} + \mathbf{R_V} + \mathbf{R_N}. \quad (6)$$

The noise cross-correlation matrix is given by $\mathbf{R_N} = \sigma_n^2\mathbf{I}$, with identity matrix $\mathbf{I}$, due to the fact that the noise is assumed to be uncorrelated across electrodes, but equal in power. The atrial cross-correlation matrix is given by

$$\mathbf{R_A} = \mathrm{E}\left[\mathbf{S}_a\mathbf{S}_a^H\right] = \mathrm{E}\left[S_a\mathbf{aa}^H S_a^H\right] = \sigma_a^2\mathbf{aa}^H, \quad (7)$$

with σ_a^2 the PSD of S_a. Similarly, we can write $\mathbf{R_V} = \sigma_v^2\mathbf{vv}^H$, with σ_v^2 the ventricular PSD. Per frequency band f, both the atrial and the ventricular cross-correlation matrices are thus assumed to be rank-1.

3.1. Ventricular transfer function

The ventricular signal component originates from relatively far away and is received instantaneously at the different electrodes, implying that the phase differences inside the VTF are negligible and the magnitude differences

are small. The first candidate estimate of the VTF will therefore be a normalized all-ones vector, i.e.,

$$\hat{\mathbf{v}}_1 = \frac{1}{\sqrt{M}}\mathbf{1}, \quad (8)$$

with all-ones vector $\mathbf{1}$. We could also try to make a better estimate of $\mathbf{v}$ by looking at the eigenvectors of $\mathbf{R_X}$ and selecting the one closest to the all-ones vector. The eigenvalue decomposition of $\mathbf{R_X}$ is given by $\mathbf{R_X U} = \mathbf{U\Lambda}$, where $\mathbf{U}$ contains the eigenvectors as its columns and where $\mathbf{\Lambda}$ is a diagonal matrix containing the eigenvalues. Because $\mathbf{R_X}$ is Hermitian, $\mathbf{U}$ is a unitary matrix, that is $\mathbf{U}^{-1} = \mathbf{U}^H$. This results in $\mathbf{R_X} = \mathbf{U\Lambda U}^H$. We assume that the VTF is given by one of the columns of $\mathbf{U}$. This eigenvector is therefore expected to be relatively similar to the all-ones vector. The second candidate estimate of the VTF is therefore obtained by the following maximization

$$\hat{\mathbf{v}}_2 = \arg\max \mathbf{U}^H\mathbf{1}. \quad (9)$$

This estimate of the VTF allows to take small variations in magnitude differences between the ventricular components as received by the different electrodes into account.

3.2. Atrial transfer function

The interfering ventricular and noise cross-correlation matrices $\mathbf{R_V}$ and $\mathbf{R_N}$ can then be used to obtain an estimate of $\mathbf{R_A}$. To do so, we can use the covariance whitening method [5], which uses the interfering cross-correlation matrices to pre-whiten the noisy $\mathbf{R_X}$.

Pre-whitening can be achieved by applying the generalized eigenvalue decomposition (GEVD) to the matrix pencils $(\mathbf{R_X}, \mathbf{R_V} + \mathbf{R_N})$ or $(\mathbf{R_A}, \mathbf{R_V} + \mathbf{R_N})$, where $\mathbf{R_X}$ can be determined from the data itself, $\mathbf{R_V}$ and $\mathbf{R_N}$ have been composed using the assumptions in the previous subsection and $\mathbf{R_A}$ is to be determined. Starting with the decomposition of the second matrix pencil, a non-singular matrix $\mathbf{U}$ and diagonal matrix $\mathbf{\Lambda}$ can be found that conform to the following two equations,

$$\mathbf{U}^H\mathbf{R_A U} = \mathbf{\Lambda} \quad \text{and} \quad \mathbf{U}^H\left(\mathbf{R_V} + \mathbf{R_N}\right)\mathbf{U} = \mathbf{I}, \quad (10)$$

where $\mathbf{U}$ and $\mathbf{\Lambda}$ contain the generalized eigenvectors and eigenvalues. Without loss of generality, we assume the generalized eigenvalues are sorted from large to small. With $\mathbf{Q} = \mathbf{U}^{-H}$, the two equations can be rewritten into

$$\mathbf{R_A} = \mathbf{Q\Lambda Q}^H \quad \text{and} \quad \mathbf{R_V} + \mathbf{R_N} = \mathbf{QQ}^H. \quad (11)$$

Summing these two expressions gives

$$\mathbf{R_X} = \mathbf{Q}\left(\mathbf{\Lambda} + \mathbf{I}\right)\mathbf{Q}^H, \quad (12)$$

which can be transformed back into

$$\mathbf{U}^H\mathbf{R_X U} = \mathbf{\Lambda} + \mathbf{I}. \quad (13)$$

Page 2

From this it follows that the GEVD of either of the two matrix pencils gives the same generalized eigenvectors. Prewhitening can thus be achieved using the GEVD. However, we only need the ATF $\mathbf{a}$. Comparing $\mathbf{R_A} = \mathbf{Q \Lambda Q^H}$ with $\mathbf{R_A} = \sigma_a^2 \mathbf{aa^H}$ shows that under the current signal model assumptions, only the first value of the diagonal of $\mathbf{\Lambda}$ is non-zero and that the ATF should therefore be captured in the first column of $\mathbf{Q}$ with a scalar ambiguity. Notice that this is a result of the assumption that $\mathbf{R_A}$ has rank-1. We can also calculate $\mathbf{Q}$ as the left eigenvectors of $(\mathbf{R_V} + \mathbf{R_N})^{-1} \mathbf{R_X}$.

4.   Atrial signal estimation

With the interfering cross-correlation matrices and the ATF and VTF known, it is possible to derive the beamformer $\mathbf{W}$ to estimate the atrial signal source s_a and therefore the atrial signal component $\mathbf{s}_a$ at each electrode m.

4.1.   Extended bipolar electrode

The BE can be interpreted as a beamformer for $M = 2$ with $\mathbf{w} = [1, -1]^H$. This can be extended to M electrodes as a subtraction of the mean of all electrodes from each electrode m. This results in the beamformer matrix $\mathbf{W} = \mathbf{I} - \frac{1}{M} \mathbf{1} \mathbf{1}^H$, which can be interpreted as a filter that estimates the ventricular component using the VTF $\hat{\mathbf{v}}_1$ and subtracts that from the EGM. Extending this to using either VTF estimate, this gives the following extended bipolar electrode (EBE) beamformer matrix,

$$\mathbf{W}_{\text{EBE}} = \mathbf{I} - \mathbf{vv}^H, \tag{14}$$

where we assume that $\mathbf{v}$ is normalized to have unit norm.

The BE results as a special case of the expression in Eq. (14) when using $M = 2$ electrodes in combination with the VTF estimate $\hat{\mathbf{v}}_1$ for $\mathbf{v}$.

4.2.   MVDR beamformer

A well known beamformer from the field of array processing is the minimum variance distortionless response (MVDR) beamformer, see e.g., [6], derived from the following minimization problem,

$$\min_{\mathbf{w}} \quad \mathbf{w}^H (\mathbf{R_V} + \mathbf{R_N}) \mathbf{w}$$
$$\text{s.t.} \quad \mathbf{w}^H \mathbf{a} = 1. \tag{15}$$

This formulation can be solved by minimizing the Lagrangian, resulting in the following beamformer matrix,

$$\mathbf{W}_{\text{MVDR}} = \frac{\left(1 + \sigma_n^2/\sigma_v^2\right) \mathbf{aa}^H - \left(\mathbf{v}^H\mathbf{a}\right) \mathbf{va}^H}{1 + \sigma_n^2/\sigma_v^2 - (\mathbf{v}^H\mathbf{a})(\mathbf{a}^H\mathbf{v})}, \tag{16}$$

where the PSD fraction σ_n^2/σ_v^2 is typically small and where $\mathbf{v}$ and $\mathbf{a}$ are assumed to be normalized to have unit norm.

5.   Simulation results

In this section we evaluate and compare the presented estimators for AA extraction with the standard BE configuration. As the true AA is unknown for clinical data, we perform a comparison based on simulated EGM data and quantify the results using instrumental quality metrics.

5.1.   Data set

The simulated EGMs are composed as described by Sun *et al.* in [7]. Similarly, we simulate EGMs with and without AF with a sampling frequency of $F_s = 1\,\text{kHz}$ and a length of $T = 5\,\text{s}$. The data is split into 500 time frames of $50\,\text{ms}$ overlapping 50%. We simulate an array of 5×5 electrodes, thus $M = 25$, on a regular grid of 90×90 simulated cells with a cell-to-cell distance of $200\,\mu\text{m}$. More details on the tissue modeling are given in [7]. The model simulates AF by adding multiple focal sources and by inserting areas of badly conducting tissue. With this simulated data, the atrial and ventricular activity are separately available.

We will consider one data set without AF, consisting of normal SR, and three data sets with an increasing degree of AF by raising the number of focal sources and inserting more areas of badly conducting tissue. All EGMs have been degraded with sensor self noise at an SNR of $20\,\text{dB}$.

5.2.   Error measure

To quantify the estimation errors on the AA and the amount of residual VA, we apply the filters, derived using the full EGMs $\mathbf{x}$, to the available separate atrial and ventricular components, that is $\hat{\mathbf{s}}_a = \mathbf{W}^H \mathbf{s}_a$ and $\hat{\mathbf{s}}_v = \mathbf{W}^H \mathbf{s}_v$. Then we calculate the atrial root-mean-square error (ARMSE) and the ventricular residual energy (VRE) with the time domain versions of those two estimates as

$$\text{ARMSE} = \|\hat{\mathbf{s}}_a[t] - \mathbf{s}_a[t]\|_2 \quad \text{and} \quad \text{VRE} = \|\hat{\mathbf{s}}_v[t]\|_2 . \tag{17}$$

For both metrics it holds that the lower the value, the better.

5.3.   Sinus rhythm

Fig. 1a shows the results in terms of VRE versus ARMSE for the reference method BE, and the two proposed methods EBE and MVDR, applied to the SR data set. The results are shown for both the VTF estimates $\hat{\mathbf{v}}_1$ and $\hat{\mathbf{v}}_2$. The curves in Fig. 1a are parameterized by the number of electrodes used in the algorithm, which means that along the curve the number of electrodes increases from 2 to 25. For both the EBE and MVDR approach it follows that increasing the number of electrodes generally improves both the estimation of the AA and the cancellation of the VA. The MVDR in combination with the VTF
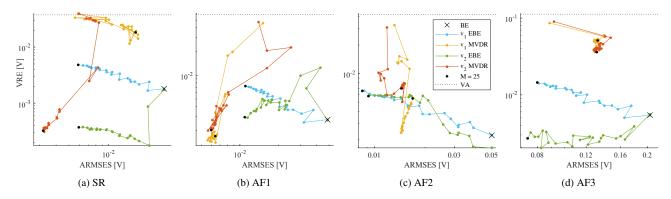
×	BE
—	v_1 EBE
—	v_1 MVDR
—	v_2 EBE
—	v_2 MVDR
•	$M = 25$
⋯	VA

(a) SR   (b) AF1   (c) AF2   (d) AF3

Figure 1: Comparison in terms of ARMSE versus VRE for all four data sets. The number of electrodes increases along the curve from $M = 2$ to $M = 25$ electrodes, where $M = 25$ is indicated with a black dot. The energy of the unfiltered ventricular signal is indicated with a dotted line.

estimate $\hat{\mathbf{v}}_2$ clearly outperforms the BE and EBE approach. Further we see that for SR, using the $\hat{\mathbf{v}}_2$ estimate over $\hat{\mathbf{v}}_1$ leads to significantly better results.

5.4.   Atrial fibrillation

Figs. 1b-1d show the performance in a similar way as in Fig. 1a, but now for the AF data sets. The results for the simplest AF data set AF1 are in line with the SR data set in Fig. 1a: The proposed MVDR-based estimator clearly improves over the BE and EBE approach. However, we also see that the large improvements of the VTF estimate $\hat{\mathbf{v}}_2$ over using the simpler $\hat{\mathbf{v}}_1$ as shown in Fig. 1a for SR seem to vanish. For the data sets AF2 and AF3, shown in Figs. 1c-1d, however, we see that the proposed EBE has the better performance over the BE and the MVDR-based approach. The reduced performance of the MVDR compared to the EBE approach is most likely due to the assumptions that are used when deriving the MVDR-based approach: assuming that $\mathbf{R_A}$ has rank-1. Most likely, during higher degrees of AF this assumption becomes less valid. The results do however show that extending the BE using more electrodes and using the $\hat{\mathbf{v}}_2$ estimate gives significantly better results than the BE.

6.   Discussion and conclusion

In this paper, we formulated the problem of atrial activity estimation as a beamforming problem and proposed two different beamformers for AA estimation. Simulations are done with synthetically generated EGMs containing both VA and various degrees of AF.

The simulations show that for an increasing number of electrodes, the performance of the two proposed beamformers increases. For data sets with a low degree of AF, the MVDR performs better than the EBE. The EBE, however, outperforms the MVDR in the two scenarios with

higher degrees of AF. This is probably due to the rank-1 assumption for the $\mathbf{R_A}$ matrix, which is harder to satisfy for higher degrees of AF. The proposed EBE always improves over the well known BE configuration.

Matlab Implementations can be downloaded from *https://cas.tudelft.nl/Repository/*.

References

[1] Stewart S, Hart C, Hole D, McMurray J. Population prevalence, incidence, and predictors of atrial fibrillation in the renfrew/paisley study. Heart 2001;86(5):516–521.

[2] Yaksh A, et al. A novel intra-operative, high-resolution atrial mapping approach. Journal of Interventional Cardiac Electrophysiology 2015;44(3):221–225.

[3] Takigawa M, Relan J, Martin R, Kim S, Kitamura T, Frontera A, Cheniti G, Vlachos K, Massoullié G, Martin CA, et al. Effect of bipolar electrode orientation on local electrogram properties. Heart Rhythm 2018;15(12):1853–1861.

[4] Benesty J, Chen J, Pan C, et al. Fundamentals of differential beamforming. Springer, 2016.

[5] Markovich-Golan S, Gannot S. Performance analysis of the covariance subtraction method for relative transfer function estimation and comparison to the covariance whitening method. In IEEE Int. Conf. Acoust., Speech and Signal Proc. 2015; 544–548.

[6] Habets EA, Benesty J, Gannot S, Cohen I. The MVDR beamformer for speech enhancement. In Speech processing in modern communication. Springer, 2010; 225–254.

[7] Sun M, de Groot NM, Hendriks RC. Joint cardiac tissue conductivity and activation time estimation using confirmatory factor analysis. Computers in Biology and Medicine 2022; 144.

Address for correspondence:

Dr. ir. Richard C. Hendriks
r.c.hendriks@tudelft.nl
Mekelweg 4, 2628 CD Delft, The Netherlands